Investigating structure, magneto-electronic, and thermoelectric properties of the new d^0 quaternary Heusler compounds RbCaCZ (Z = P, As, Sb) from first principle calculations

S Gheriballah[a,*], B Bouabdellah[a], A Oughilas[a], M A Boukli[a], M Rahmoune[a] & A Sayede[b]

[a]Condensed Matter & Sustainable Development Laboratory (LMCDD), University of Sidi Bel-Abbes, Sidi Bel-Abbes 22000, Algeria
[b]UCCS, CNRS-UMR 8181, Université d'Artois, Faculté des Sciences Jean Perrin, Rue Jean Souvraz, SP 18, 62307 Lens Cedex, France

The *ab initio* calculations based on the density functional theory (DFT) using the self-consistent full potential linearized augmented plane wave (FPLAPW) method were performed to explore the electronic structures, magnetic and thermoelectric properties of quaternary alloys RbCaCZ (Z = P, As, Sb) with quaternary Heusler structure. Results showed that FM-Y3 is the most favorable atomic arrangement. All the compounds are found to be half-metallic ferromagnetic materials with an integer magnetic moment of 2.00 μ_B, which predominantly derives from the strong spin polarization of p channels of C hybridized with Z elements. The predicted minority (half-metallic) band gaps were found to be 1.86 (0.87), 1.72 (0.78), and 1.78 (0.71) eV for Z = P, As, and Sb, respectively. Thermoelectric properties of the RbCaCZ (Z = P, As, Sb) materials are additionally computed over an extensive variety of temperature and it is discovered that all compounds demonstrates higher figure of merit. The half-metallic structures of these compounds with large band gaps and adequate Seebeck coefficients mean that they are suitable for use in spintronic and thermoelectric device applications.

Keywords: *Q*uaternary Heusler compounds; Electronic structures; Magnetic properties; Half-Metals; Thermoelectric properties

1 Introduction

Human activities, automotive exhaust, industrial processes and emission of CO_2 are causing adverse climate changes. Thermoelectric (TE) materials play an important role in global sustainable energy solution. These materials are investigated not only owing to their high potential of converting directly waste thermal energy to useful electrical energy but also to their capability to reduce effectively the environmental pollution. In recent decades, quaternary Heusler alloys have attracted much interest due to their low toxicity and their excellent properties such as half-metallic ferromagnetism (HMF) and high thermoelectric performance, where they have possible uses in spintronic and thermoelectric applications[1-4]. Based on chemical composition, Heusler alloys are grouped into three types: (a) full-Heusler with compositional formula of X_2YZ where X and Y are transition metals and Z is *sp* element. These alloys crystallize in *L21*-type structure. The symmetric operations followed are either of *Fm3m* space group with prototype structure Cu_2MnAl or of *F43m* space group with Hg_2CuTi as a

model structure. The alloy crystallizes in lateral prototype only when numbers of valence electrons of Y are larger than X. (b) half-Heusler alloy, with *C1b* structure having *F43m* symmetry. These can be obtained from X_2YZ type by keeping one of the X sites vacant. The compositional formula then becomes XYZ. (c) Quaternary Heusler alloys (QHAs) are derived from full-Heusler alloys by replacing one of X atoms with different transition metal atoms X′. The chemical formula of QHAs is XX′YZ.

However, different from traditional magnetic Heusler materials containing unpaired *d* or *f* electrons, many works have revealed that Heusler compounds without transition metal elements, *sp* or d^0 compounds, with ternary half-Heusler structure[5-8] and full-Heusler structure[9-12] would be a new type of HM materials where the spin polarization and magnetic order are mainly from the anion *p*-electrons of anions. However, research and report on d^0 HM compounds with quaternary Heusler structure are still rare[13-17]. To the best of our knowledge, up to now, no study on HM and thermoelectric properties for our d^0 quaternary Heusler compounds RbCaCZ (Z = P, As, Sb) has been reported in the literature.

_____
*Corresponding author: (E-mail:gheriballahslimane@gmail.com)

In this paper, the structural, electronic, magnetic and thermoelectric properties of new quaternary d^0 Heusler compounds RbCaCZ (Z = P, As, Sb) have been studied by using the first-principles calculations. The characteristics of energy bands and origin of half-metallic gap were studied. Also the thermoelectric properties of RbCaCZ (Z = P, As, Sb) compounds such as Seebeck coefficient, electrical and thermal conductivity in the large temperature range are discussed. We have chosen this series of compounds with the hope that they would exhibit half-metallicity, good magnetic and thermoelectric properties and they may help experimentalists to design new efficient thermoelectric materials. Our paper is organized as follows. The theoretical background is presented in Sec. 2. Results and discussion are presented in Sec. 3. A summary of the results is given in Sec. 4.

2 Computational Method

The calculations of the present study of the alloy RbCaCZ (Z = P, As, Sb) are performed in the framework of the density functional theory (DFT)[18]. The electronic structure were carried out using the full-potential linearized augmented plane wave (FP-LAPW) method based on the local spin density approximation method[19] implemented in the WIEN2k package[20]. The exchange-correlation potential was treated under the generalized gradient approximation (GGA)[21]. The convergence of the basis set was controlled by a cutoff parameter $R_{mt} . K_{max}$ = 8. A $20 \times 20 \times 20$ k-point mesh was used as base for the integration in the first Brillouin zone was found to be sufficient in most cases. The energy and charge convergence criteria were strictly set to 10^{-5} to improve accuracy in the spin-polarized calculations.

3 Results and Discussion

In general, the structural prototype of the quaternary Heusler compounds – LiMgPdSb – is denoted as Y (space group *216*)[22]. There are three non-equivalent atomic configurations for these quaternary Heusler compounds XX'YZ: *Y1*:X (0, 0, 0),X'(0.25, 0.25, 0.25), Y (0.5, 0.5, 0.5), and Z(0.75, 0.75, 0.75); *Y2*: X (0, 0, 0), X'(0.5, 0.5, 0.5), Y(0.25, 0.25, 0.25), and Z(0.75, 0.75, 0.75); *Y3*: X(0.5, 0.5, 0.5), X'(0, 0, 0), Y (0.25, 0.25, 02.5), and Z (0.75, 0.75, 0.75). In order to confirm the structural and magnetic ground states of *Y1*, *Y2* and *Y3* configuration, the total energies of the non-magnetic (NM) and ferromagnetic (FM) states as a function of the lattice constant of the three compounds were calculated and the obtained curves are shown in Fig. 1. The results show that *FM-Y3* state is the ground state structure.

In Table 1, we report our calculated equilibrium lattice constant a_0, along with the bulk modulus B_0, and the total energy E_{tot} in their different structural and magnetic configurations. As can be seen, the lattice constants increase with increasing the covalent radius of Z anion from P (7.05 Å) → As (7.18 Å) → Sb (7.41 Å). Also, with increasing lattice constant along P → As → Sb, B decreases indicating that compressibility increases and the substance gets softer. As no experimental or theoretical lattice constant, bulk modulus and total energy per formula unit have been reported, we note that ours predictive results stays in good agreement with other theoretically works for the near family of quaternary d^0 alloys excluding transition metals[13-17] suggesting that the formalism adopted in the present work is fairly accurate. Based on this, all the
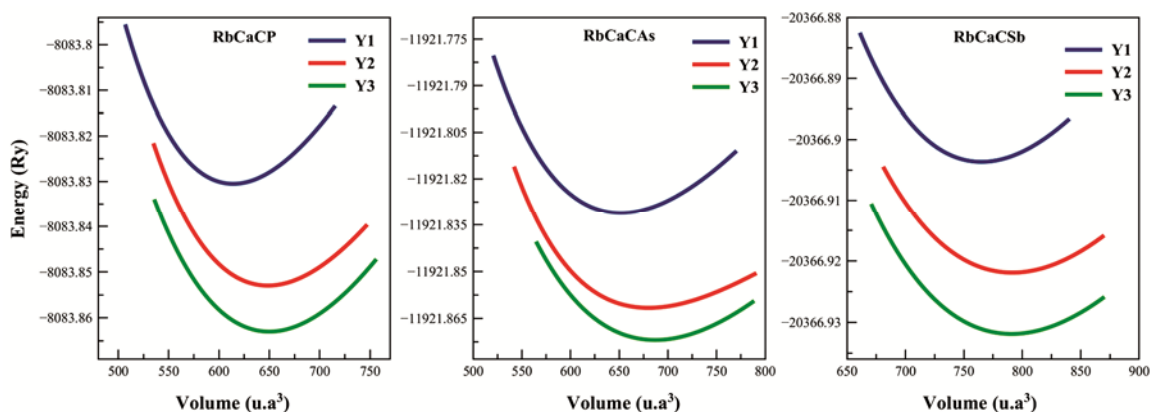

Fig. 1 — Total energy as a function of volume per formula unit (f.u.) in the type *FM-Y1*, *FM-Y2* and *FM-Y3* for the RbCaCZ (Z = P, As, Sb) compounds.

further calculations on electronic, magnetic and thermoelectric properties of RbCaCZ (Z = P, As, Sb) were performed on in the type *FM-Y3* structure.

It is well known that the band structure is vital for determining the thermoelectric properties because these properties depend greatly on the band structure. The calculated spin polarized band structures of

Table 1 — Calculated total energies E_{tot} (Ry) per formula unit, equilibrium lattice constant a_0 (Å), the bulk modulus B (GPa) for RbCaCZ (Z=P, As, Sb) compounds in theirs different structures type and magnetic configurations.

Compound	structure	E_{tot}		a_0	B_0
		NM	FM	FM	FM
RbCaCP	Type-Y1	-8083.758	-8083.830	7.05	37.2
	Type-Y2	-8083.775	-8083.853	7.27	33.12
	Type-Y3	-8083.794	-8083.863	7.28	32.73
RbCaCAs	Type-Y1	-11921.758	-11921.831	7.18	35.01
	Type-Y2	-11921.785	-11921.862	7.34	25.62
	Type-Y3	-11921.795	-11921.872	7.42	30.58
RbCaCSb	Type-Y1	-20366.835	-20366.903	7.41	30.42
	Type-Y2	-20366.885	-20366.922	7.74	26.31
	Type-Y3	-20366.895	-20366.932	7.77	25.88

RbCaCZ (Z = P, As, Sb) compounds with *FM-Y3* type configuration have been illustrated in Fig. 2. As it can be seen, the general band structures of are similar for our compounds. The results of the band structures of RbCaCZ (Z = P, As, Sb) compounds show that spin-up channels are conducting where the C-*p*-like bands passing through the Fermi level can be found, exhibiting a conducting characteristic, while spin-down channels are insulating with a indirect forbidden band gap Eg (W-Δ) around the Fermi level of 1.86, 1.72 and 1.78 eV, respevtively, confirming that these compounds are half metallic (HM). There are considerable HM gaps (E_{HM}), which are generally defined as the minimum of E_{bc} and E_{tv}, where E_{bc} is defined as the bottom energy of spin-down conduction bands with respect to the Fermi energy (E_F) and E_{tv} the absolute values of the top energy of spin-down valence bands. The large predicted half-metallic gap E_{HM} is known to be essential to describe the high stability of HM magnetism of a half metal[23]. As shown in Table 2, RbCaCP, RbCaCAs and RbCaCSb display large HM gaps of 0.87, 0.78, and
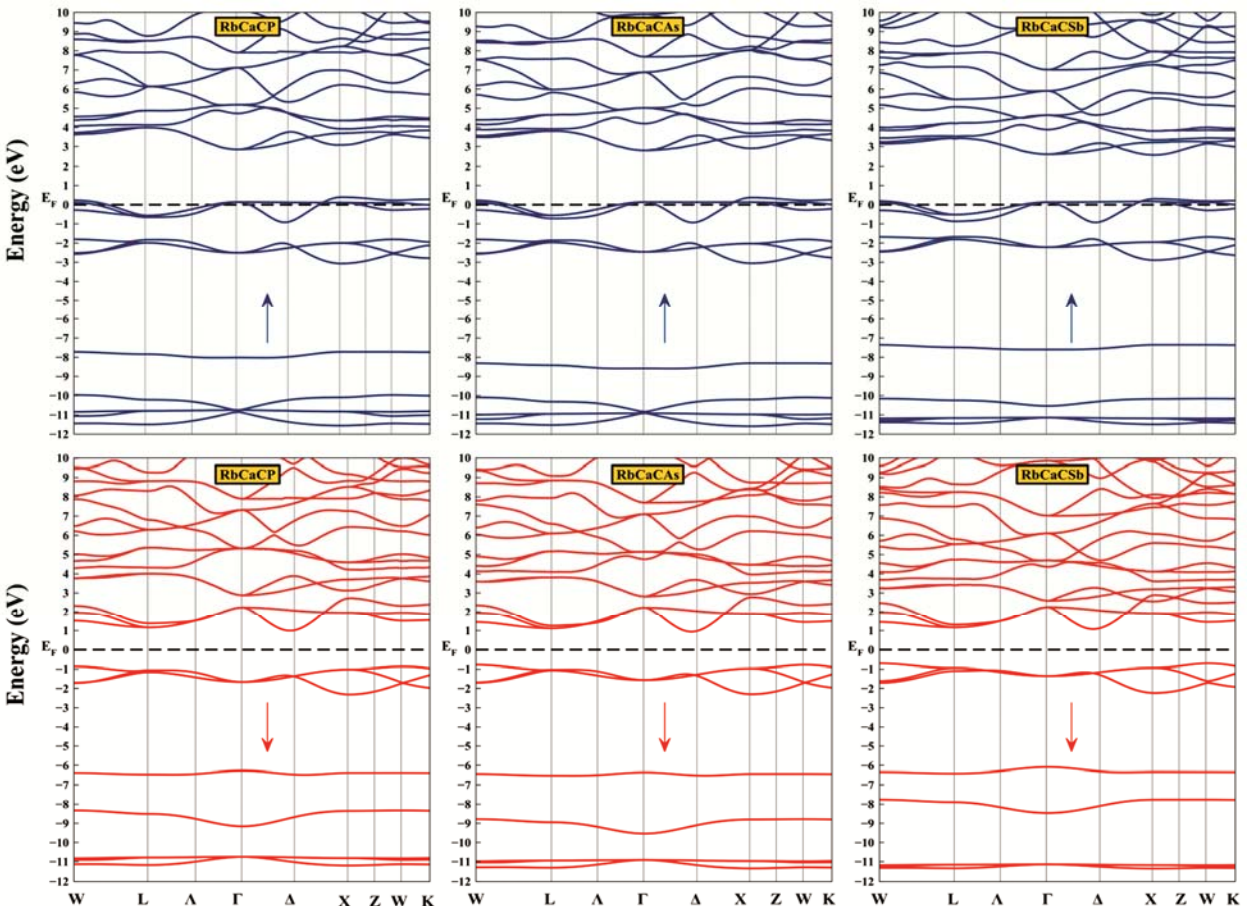

Fig. 2 — Spin polarized band structure for the RbCaCZ (Z = P, As, Sb) compounds at their equilibrium lattice constant.

0.71 eV, respectively, illustrating stable HM features. Unfortunately, so far, no experimental measurements and theoretical data band gaps E_g and E_{HM} for the investigated compounds are carried out to compare with. However, our results are in good agreement with these of the quaternary Heusler RbCaNZ (Z = O, S, Se) alloys[17] and higher than those of other quaternary Heusler d^0 alloys[13-16].

Afterward, the characteristic of energy bands in RbCaCP, as a representative of the three compounds, are investigated in detail. The three bands between -12 and -11 eV in majority spin state (around -11 eV in minority spin states) arise from Rb p states. The upper

Table 2 — The semiconducting gap E_g (eV), the half-metallic gap E_{HM} (eV), total magnetic moment μ_{tot} (μ_B), magnetic moment per atom (Rb, Ca, C, P, As, Sb) and magnetic moment in the interstitial region μ_{int} in compounds RbCaCZ (Z= P, As, Sb).

Compound	E_g	E_{HM}	μ_{tot}	μ_{Rb}	μ_{Ca}	μ_C	μ_Z	μ_{int}
RbCaCP	1.86	0.87	2	0.018	0.035	1.965	-0.3	0.282
RbCaCAs	1.72	0.78	2	0.014	0.03	1.93	-0.234	0.26
RbCaCSb	1.78	0.71	2	0.007	0.018	1.92	-0.17	0.225

single band between -11 and -10 eV in majority spin state state (between -9 and -8 eV in minority spin state) belong to P s states. The single band around -8 eV in majority spin state (between -7 and -6 eV in minority spin state) is relative to C s states. In majority spin states, the three bands between -3 and -2 eV are relative to C p, while the three bands crossing the Fermi level belong to C p. Therefore, the C p state is the main origin of the absolute spin polarization. In minority spin states, the three fully-filled bands between -2 and -1 eV are relative to P p, while the three bands above the Fermi level mainly result from the unoccupied C p tates with a small contribution from the Rb and Ca d states. A similar trend is observed in RbCaCAs and RbCaCSb alloys. In order to understand the electronic structure further and because they are similar, only calculated total and partial density of states (DOS) for the RbCaCP compound are presented in Fig. 3. The DOSs also confirm that spin-up states are semiconducting and spin-down states are metallic, which is in consistent with the data of band structures. From partial DOS,
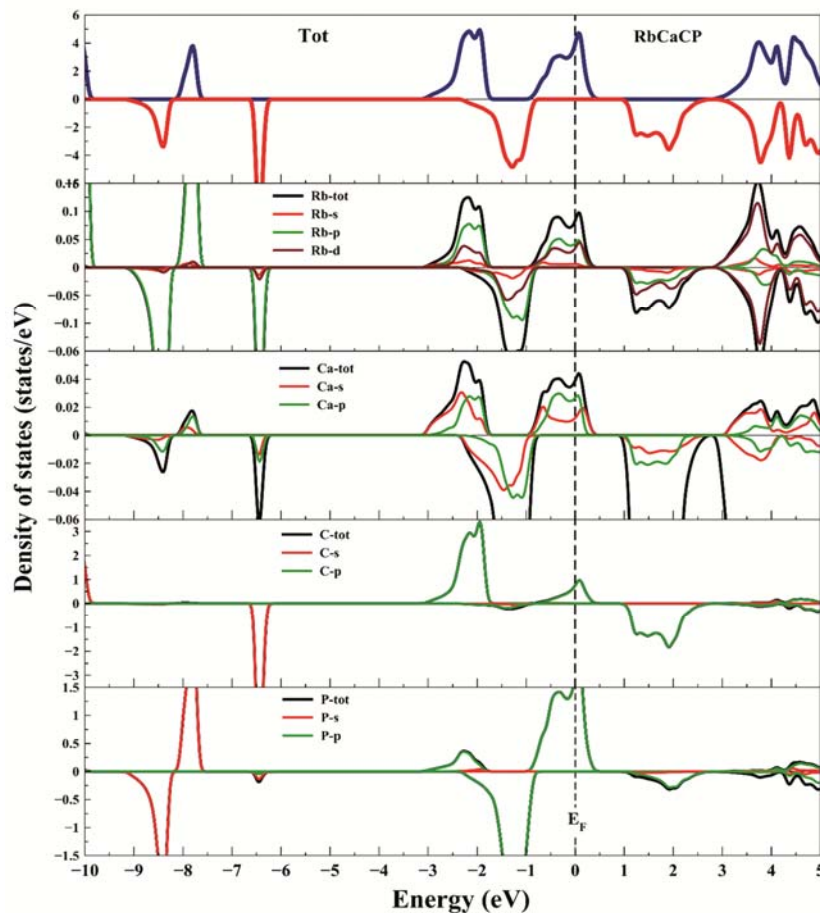

Fig. 3 — Spin-polarized total and partial denities of states (DOS) for the RbCaCP compound.

the spin state across the Fermi level is mainly from *C-p* states with smaller contribution coming from the *P*-, *As*-, and *Sb-p* states. For the spin-down states, the top of the valence bands is mainly from the P *p* states, while the bottom of the conduction bands is mainly from the *C-p* states responsible for gap formation. As can be seen, a relatively strong hybridization between C *p* and P *p* states, makes that majority spin states locate at the Fermi level, and in minority spin state the Fermi level, locates within a band gap. Furthermore, the exchange splitting effect, which is mainly observed in C *p* states, pushes spin majority states above the Fermi level and moves minority spin states below the Fermi level. This effect makes the Fermi level cross the majority spin states and fall within a band gap in minority spin state. Therefore, two factors of *p-p* hybridization and exchange splitting effect are responsible for half-metallicity.

Our total magnetic moment μ_{tot} per formula unit calculated are found to be integer value $2.00\mu_B$ for all compounds and this integer value is also a typical HM characteristic. Since the spin-down channel is completely filled with six electrons and spin-up channel is partially filled with four electrons, in principle, the total net magnetic moment of 2 μ_B is from the remaining two holes. We also list in Table 2 the local magnetic moments at the Rb, Ca, C, and Z (Z = P, As, Sb) sites. From Table 2 and for all three half-metal compounds, the main contribution to the total magnetic moment is from *p* states of C. Since the spin-down channel is completely filled with six electrons and spin-up channel is partially filled with four electrons, in principle, the total net magnetic moment of 2 μ_B is from the remaining two holes. From RbCaCP to RbCaCAs to RbCaCSb, the partial magnetic moments of Z atoms decrease because the localization of *p* states decreases from 3*p* to 4*p* to 5*p* blocks. The same tendency is observed in the others d^0 quaternary Heusler alloys[13-17].

The thermoelectric performance of a material is determined by figure of the band structure near the Fermi level and the band gap is very useful in obtaining reliable transport properties in thermoelectric materials. Thermoelectric (TE) materials transform the waste heat energy into usable electric energy, and thereby offer a possible solution to the present day energy crisis. This category of materials is currently being investigated at faster rates than the other technologically important materials

because of their ecofriendly and efficient energy management[24]. Recently, many quaternary Heusler thermoelectric materials including transition metals have been widely studied[1,25-27] but any quaternary Heusler thermoelectric materials excluding transition metals or d^0 compounds have been studied. In this study and for the first time, the thermoelectric properties of RbCaCZ (Z = P, As, Sb) compounds are calculated by the BoltzTrap code with a dense *k*-mesh of $50 \times 50 \times 50$[28].

For this, we have calculated the electrical conductivity σ/τ, thermal conductivity κ/τ, Seebeck coefficient *S* and figure of merit *ZT*. An efficient thermoelectric material is required to have high electrical conductivity, low thermal conductivity and a large Seebeck coefficient. The temperature variation of electrical conductivity (σ/τ) is reported in Fig. 4(a). We can see that electrical conductivity decreases in spin up state which confirms the metallic behavior in spin up state while in spin down state it increases with increase in temperature confirming the semiconducting behavior and thus supports the band structure.

The electronic thermal conductivity κ/τ as a function of temperature is represented in Fig. 4(b). From Fig. 4(b), we observe that for spin up states, κ/τ increases smoothly for all materials, while for spin down states, it increases tediously. The Seebeck coefficients for RbCaCZ (Z = P, As, Sb) compounds are displayed as a function of temperature in Fig. 4(c). The observed value of the Seebeck coefficient for all compounds are positive in spin up channel, signifying the presence of holes as charge carriers (*p-type*), while in spin down channel, negative value of *S* suggests electrons as charge carriers (*n-type*).

We also computed the total Seebeck coefficient *S* variation calculated by two-current model[29] to designate its nature as shown in Fig. 5(a). Comparing the plots of Seebeck coefficient for both the spin configurations and total *S*, it is clear that the spin-down channel Seebeck coefficient is dominant in all the cases. Therefore, the RbCaCZ (Z = P, As, Sb) are *n*-type materials. The sharp increase in the *S* value at lower temperatures (< 200K) indicates the presence of a low carrier concentration. In the range of temperature (200-1000K), we see a slight linear decreases of the absolute value *S*, and at 1000 K attains a value of -416, -400 and -465 $\mu V.K^{-1}$ for RbCaCP, RbCaCAs, RbCaCSb, respectively.
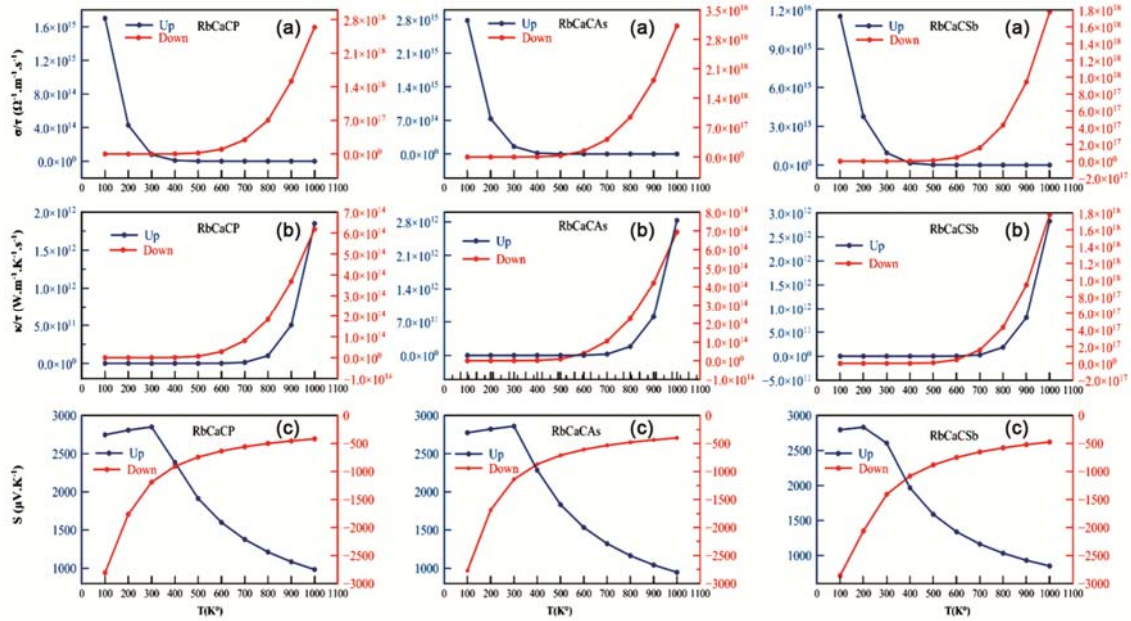
Fig. 4 — The variation of electrical conductivity σ/τ (a), thermal conductivity κ/τ (b) and Seebeck coefficient S (c) versus temperature in both the spin states for RbCaCZ (Z = P, As, Sb)
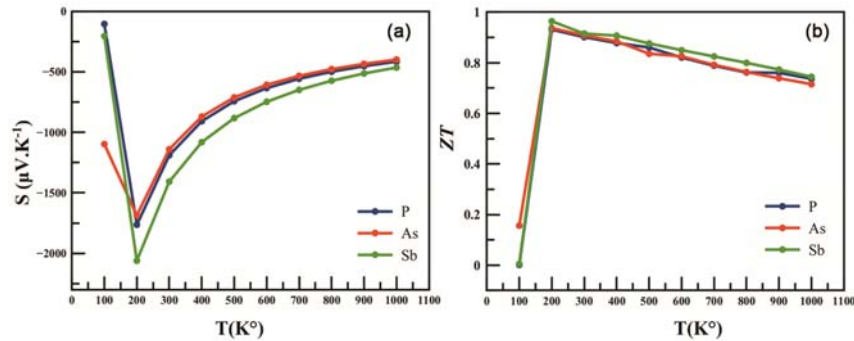

Fig. 5 — The variation of total Seebeck coefficient S (a) and figure of merit *ZT* (b) as a function of temperature for RbCaCZ (Z = P, As, Sb)

The thermoelectric performance is characterized by dimensionless figure of merit *ZT* defined as $ZT = (S^2 . \sigma . T / \kappa)$. The calculated thermoelectric figure of merit at different temperature is presented in the Fig. 5(b). The material is considered as good element for thermoelectric devices if his *ZT* is about or greater than unity[30]. The maximum thermoelectric figure of merit for is 0.932, 0.937, 0.964 at 200 K for RbCaCP, RbCaCAs, RbCaCSb, respectively corresponding to the maximum of the Seebeck coefficient *S* (see Fig. 5(a)). Higher values obtained of the figure of merit over the large temperature range suggest the good thermoelectric performance of our quaternary Heusler compounds and they could be promising materials for applications in thermoelectric generators. The value of electrical conductivity, thermal conductivity, Seebeck coefficient and figure of merit *ZT* at room temperature are summarized in Table 3. These

Table 3 — Values of electrical conductivity σ/τ (10^{13} $\Omega^{-1}.m^{-1}.s^{-1}$), thermal conductivity κ/τ (10^{10} $W.m^{-1}.K^{-1}.s^{-1}$) and Seebeck coefficient S ($\mu V.K^{-1}$), and figure of merit ZT at 300 K for RbCaCZ (Z = P, As, Sb) compounds compared with values for other quaternary Heusler alloys including transition metals

Compound	σ/τ	κ/τ	S	ZT
RbCaCP	4.5	2.12	-1190	0.901
RbCaCAs	9.5	4.1	-1140	0.908
RbCaCSb	0.63	0.41	-1408	0.916
CoFeCrAs[a]			-40	
CoFeCrSb[a]			-20	
CoFeCrSi[a]			-15	
ZnFeTiSi[b]			539.2	
CoVTiAl[c]			37.26	0.57
CoMnTiAl[d]			31	0.4
FeMnTiAl[d]			20	0.7
[a]Ref.1, [b]Ref.25, [c]Ref.26, [d]Ref.27				

materials show higher efficiency for thermoelectric relatively in comparison for the other quaternary Heusler compounds including transition metals[1,25-27].

4. Conclusion

In summary, we have predicted a series of new d^0 quaternary Heusler compounds RbCaCZ (Z = P, As, Sb) and studied the structural, electronic, magnetic and transport properties by using first-principles calculations. We found that type *FM+Y3* is the most appropriate configuration with the lowest total energy. The results show that our compounds are half-metallic ferromagnets at equilibrium lattice constant with a large and robust half-metallic gap E_{HM}. Also the transport properties of the material reveal some fruitful results. These materials exhibit high values of Seebeck coefficient and figure of merit at room temperature. The overall properties envisioned confirm that all these alloys can find applications in thermoelectric and spintronic applications. We expected that the present theoretical estimation of various physical parameters can prove as valuable reference for future experimental work.

References

1 Bhat T M & Gupta D C, *J Magn Magn Mater*, 449 (2018) 493.
2 Elahmar M H, Rached H, Rached D, Khenata R, Murtaza G, Bin O S & Ahmed W K, *J Magn Magn Mater*, 393 (2015) 165.
3 Benkabou M, Rached H, Abdellaoui A, Rached D, Khenata R, Elahmar M H, Abidri B & Benkhettou N, Bin-Omran S, *J Alloys Compd*, 627 (2015) 276.
4 Hossain M A, Rahman M T, Khatun M & Haque E, *Comput Condens Matter*, 15 (2018) 31.
5 Benaissa H, Benatmane S, Amari S & Obodo K O, *Spin*, 8 (2018) 1850008.
6 Yao K L, Jiang J L, Liu Z L & Gao G Y, *Phys Lett A*, 359 (2006) 326.
7 Volnianska O & Boguslawski P, *J Phys: Condens Matter*, 22 (2010) 073202.
8 Chen J, Gao G Y, Yao K L & Song M H, *J Alloys Compd*, 509 (2011) 10172.
9 Wei X P, Chu Y D, Sun X W, Deng J B & Xing Y Z, *Superlattice Microstruct*, 74 (2014) 70.
10 Rozale H, Lakdja A, Amar A, Chahed A & Benhelal O, *Comput Mater Sci*, 69 (2013) 229.
11 Zhang L, Wang X T, Rozale H, Lu J W & Wang L Y, *J Supercond Nov Magn*, 28 (2015) 3701.
12 Ahmad M, Naeemullah, Murtaza G, Khenata R, BinOmran S, & Bouhemadou A, *J Magn Magn Mater*, 377 (2015) 204.
13 Du J, Dong S, Wang X T, Zhao H, Wang L Y & Feng L F, *AIP Adv*, 6 (2016) 105308.
14 Du J, Dong S, Lua Y L, Zhao H, Feng L F & Wang LY, *J Magn Magn Mater*, 428 (2017) 250.
15 Du J, Dong S, Wang X T, Rozale H, Zhao H, Wang L Y & Feng L F, *Superlattices Microstruct*, 105 (2017) 39.
16 Bouabça A, Rozale H, Amar A, Wang X T, Sayade A & Chahed A, *J Magn Magn Mater*, 419 (2016) 210.
17 Rezaei S & Ahmadian F, *J Magn Magn Mater*, 456 (2018) 78.
18 Hohenberg P & Kohn W, *Phys Rev B*,136 (1964) 864.
19 Wimmer E, Krakauer H, Weinert M & Freeman A J, *Phys Rev B*, 24 (1981) 864.
20 Blaha P, Schwarz K, Madsen G K H, Kvasnicka D & Luitz J, WIEN2k An Augmented Plane Wave Local Orbitals Program for Calculating Crystal Properties, Technische Universität, Wien, 2001.
21 Perdew J P, Burke S & Ernzerhof M, *Phys Rev Lett*, 77 (1996) 3865.
22 Dai X, Liu G, Fecher G H, Felser C, Li Y & Liu H, *J Appl Phys*, 105 (2009) 07E901.
23 Şasioğlu E, Sandratskii L M & Bruno P, *J Phys: Condens Matter*, 17 (2005) 995.
24 Khandy S A & Gupta D C, *J Magn Magn Mater*, 441 (2017) 166.
25 Lin T T, Gao Q, Liu G D, Dai X F, Zhang X M & Zhang H B, *Current Appl Phys*, 19 (2019) 721.
26 Yousuf S & Gupta D C, *Mater Sci Eng B*, 221 (2017) 73.
27 Bhat T M & Gupta D C, *RSC Advances*, 6 (2016) 80302.
28 Madsen G K H & Singh D J, *Phys Commun*, 175 (2006) 67.
29 Xiang H J & Singh D J, *Phys Rev B*, 76 (2007) 195111.
30 Takeuchi T, *Mater Trans*, 50 (2009) 2359.